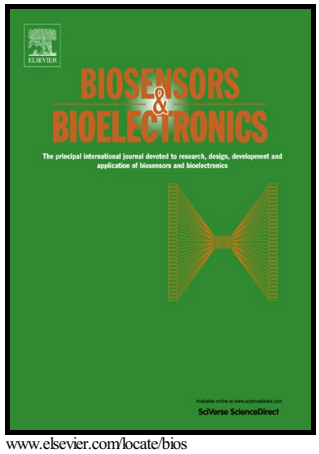

www.elsevier.com/locate/bios

Graphene and Au NPs co-mediated enzymatic silver deposition for the ultrasensitive electrochemical detection of cholesterol

Yong Huang, Jie Tan, Lijie Cui, Zhide Zhou, Zhenghua Zhang, Rong Zheng, Yewei Xue, Mengxin Zhang, Shanshan Li, Nixuan Zhu, Jintao Liang, Guiyin Li, Sufang Zhou, Yongxiang Zhao

PII: S0956-5663(17)30766-2
DOI: https://doi.org/10.1016/j.bios.2017.11.037
Reference: BIOS10113

To appear in: *Biosensors and Bioelectronic*

Received date: 29 July 2017
Revised date: 8 November 2017
Accepted date: 9 November 2017

Cite this article as: Yong Huang, Jie Tan, Lijie Cui, Zhide Zhou, Zhenghua Zhang, Rong Zheng, Yewei Xue, Mengxin Zhang, Shanshan Li, Nixuan Zhu, Jintao Liang, Guiyin Li, Sufang Zhou and Yongxiang Zhao, Graphene and Au NPs co-mediated enzymatic silver deposition for the ultrasensitive electrochemical detection of cholesterol, *Biosensors and Bioelectronic,* https://doi.org/10.1016/j.bios.2017.11.037

Graphene and Au NPs co-mediated enzymatic silver deposition for the ultrasensitive electrochemical detection of cholesterol

Yong Huang [1, 2, a], Jie Tan[1, a], Lijie Cui[2, a], Zhide Zhou[2], Zhenghua Zhang[1], Rong Zheng[1], Yewei Xue[2], Mengxin Zhang[1], Shanshan Li[2], Nixuan Zhu[2], Jintao Liang[2], Guiyin Li[1, 2*], Sufang Zhou[1*], Yongxiang Zhao[1*]

[1]National Center for International Research of Biological Targeting Diagnosis and Therapy, Guangxi Key Laboratory of Biological Targeting Diagnosis and Therapy Research, Collaborative Innovation Center for Targeting Tumor Diagnosis and Therapy, Guangxi Medical University, Nanning, Guangxi 530021, China

[2]School of Life and Environmental Sciences, Guilin University of Electronic Technology, Guilin, Guangxi 541004, China

[a]These authors contributed equally to this work.

*Corresponding author: yongxiang_Zhao@126.com (Y. Zhao)

liguiyin01@163.com (G.Y. Li)

zsf200000@163.com (S. Zhou)

Tel: +86-771-5317175；Fax: +86-771-5317175

Abstract

Cholesterol is an essential ingredient in mammals, and serum cholesterol is a major component of atherosclerotic plaques. The level of cholesterol in human serum has become an important index for clinical diagnosis and prevention of cardiovascular disease. In this paper, a simple and ultrasensitive cholesterol biosensor based on graphene oxide (GO) and gold nanoparticles (Au NPs) co-mediated enzymatic silver deposition was designed by immobilizing cholesterol oxidase (CHOD), cholesterol esterase (CHER) and GO onto the surface of Au NPs modified screen-printed carbon electrode (SPE). Under the synergistic effect of CHER, CHOD and GO, the cholesterol was hydrolyzed to generate hydrogen peroxide, which can reduce the silver (Ag) ions in the solution to metallic Ag which deposited on the surface of Au NPs modified SPE. The ultrasensitive detection of cholesterol was achieved by anodic stripping voltammetry measurement of the enzymatically deposited Ag. Under optimal conditions, the anodic stripping peak current of Ag increased with the increasing cholesterol concentration in the range from 0.01μg/mL to 5000 μg/mL with a limit of detection of 0.001 μg/mL (S/N=3). In addition, the ultrasensitive cholesterol biosensor exhibited higher specificity, acceptable reproducibility and excellent recoveries for cholesterol detection.

Key words: Cholesterol biosensor; Graphene; Enzyme catalyzed silver deposition; Screen-printed carbon electrode; Gold nanoparticles

1. Introduction

Cholesterol is a waxy steroid metabolite substance found in fat, blood, and cells in the human and higher animals, which is not only a component of cell membrane but also a starting material for the synthesis of bile acid, vitamin D and steroid hormones (Bui and Park 2016; Li et al. 2012). As a part of a healthy dietary intake of fats, cholesterol plays an important role in the brain, nervous and immune systems of humans. The level of cholesterol in human serum has become an important index for clinical diagnosis and prevention of cardiovascular disease (Batra et al. 2015; Cao et al. 2013). The serum cholesterol level in healthy human is less than 5.17 mmol/L and it has quite a few interfering species like glucose, uric acid and ascorbic acid because of nearby redox potentials (Alexander et al. 2017). High levels of cholesterol in blood can lead to a risk for heart disease, because the molecules that transport cholesterol can damage arteries and cause blockages, while low levels of cholesterol may also cause diseases such as hypolipoproteinemia, hyperthyrea, septicaemia and malnutrition (Tig et al. 2016). Consequently, sensitive and accurate detection of cholesterol is of great importance in the diagnosis and prevention of diseases.

Until now, several methods have been reported for the detection of cholesterol, such as colorimetric method, spectrophotometry, thin layer chromatography, gas-liquid chromatography, fluorimetric method, polarographic method and gas chromatography/mass spectrometry (Abraham et al. 2015; Khatun et al. 2017; Lin et al. 2017). These methods involved sophisticated procedures for the precipitation of lipoproteins and expensive equipments, or lacked of sensitivity and selectivity (V and Berchmans 2016). Thus, it is important to develop a high sensitivity and low cost method for the detection of cholesterol.

At present, electrochemical biosensor has gained more attention owing to its portability,

sensitivity, efficiency and accuracy. Electrochemical cholesterol biosensors offer the advantages such as specific recognition of cholesterol, low cost and rapid quantification (Komathi et al. 2016; Lin et al. 2016; Nandini et al. 2016). For instance, Lin et al (Lin et al. 2016) had constructed a sensitive biosensor, Chox/MoS2-AuNPs/GCE, to analyze the cholesterol with a limit of detection (LOD) of 0.26 ± 0.015 μmol/L.

Graphene, a novel 2D honeycomb-like structure of a monolayer of sp2-bonded carbon atoms (Bo et al. 2017), has gained great interest in electrochemical sensors owing to its large specific surface area, fast heterogeneous electron-transfer rate, excellent water-solubility, rich functional groups and good biocompatibility (Lee et al. 2015; Yee et al. 2016). Graphene-based nanomaterials could offer a unique feature for the fabrication of biosensors (Bai et al. 2016; Halder et al. 2017). Sharma and Mobin (Sharma and Mobin 2017) had demonstrated a peroxidase mimic CuO: graphene nanosphere composite (CuO:GNS) as colorimetric dual sensor for hydrogen peroxide and cholesterol detection. The nano-composite sensor has shown a linear response for cholesterol in the range of 0.1 - 0.8 mmol/L with LOD as low as 78 μmol/L. Furthermore, graphene has brought another revolution in the scientific frontier in terms of improving performance in various electrochemical applications (Sharma et al. 2017; Zheng et al. 2016). More importantly, it is recently reported that the graphene can effectively catalyze the deposition of silver nanoparticles (Ag NPs) due to the intrinsic reduction characteristic and rich active groups of graphene (Gao et al. 2017; Wan et al. 2011).

The evaluation of sensitive electrochemical detection strategy often requires noise reduction and signal amplification to attain sufficient reproducibility and low detection limit. Enzyme-catalyzed deposition of Ag NPs has shown promising applications as an effective way to reduce background and push down the detection limit, owning to the high catalytic activity for biochemical reactions, in

situ high efficient enzymatic catalysis of Ag NPs deposition and the increase of conductivity resulted by Ag deposition (Chen et al. 2016; Conzuelo et al. 2016; Yang and Gao 2015). Jiaul Haque et al (Jiaul Haque et al. 2015) had developed a novel enzymatic Ag-deposition scheme combined with chemical-chemical redox cycling by reduced β-nicotinamide adenine dinucleotide for the sensitive detection of creatine kinase-MB with LOD of 10 pg/mL. Recently, our group (Huang et al. 2017) had developed an electrochemical cholesterol biosensor based on enzymatic Ag deposition on Au NPs modified SPE with the LOD of 3.0 μg/mL.

In this work, we demonstrated a ultrasensitive and selective assay for cholesterol analysis which used GO and Au NPs co-mediated Ag deposition for signal amplification. The prepared cholesterol biosensor was characterized with CV, SEM, XPS and Raman spectra. Several assay conditions, such as the concentration of silver ion, incubate temperature, the concentration of GO, the immobilization time of enzyme and the pH value of the detection solution, were optimized to obtain the excellent analytical performance.

2. Materials and methods

2.1 Chemicals and reagents

Cholesterol oxidase (CHOD), cholesterol esterase (CHER), cholesterol, 1-ethyl-3-(3-dimethyl-aminopropyl)carbodiimide (EDC) and N-hydroxysuccinimide (NHS) were purchased from Sigma-Aldrich Company (St. Louis, MO, USA). Glycine, $HAuCl_4$, glucose, and DL-cysteine, ascorbic acid, bull serum albumin (BSA), and uric acid were supplied by Sangon Biotech (Shanghai, China). Graphene oxide (GO) was purchased from Xianfeng Nano Materials Tech Co. Ltd. (Nanjing, China). All other reagents were of analytical grade and used without further purification. All solutions were prepared with ultrapure water of 18.0 MΩ·cm purified from a Milli-Q purification system (Milli-Pore,

Bedford, MA, USA).

Glycine buffer solution (GBS, 0.05 mol/L, pH 8.6) was prepared by dissolving the glycine into ultrapure water and the pH value was adjusted to 8.6 using 0.1 mol/L NaOH.

A stock cholesterol solution (2.0 mg/mL) was prepared by dissolving 4.0 mg cholesterol into a mixture solution of 0.2 mL isopropanol and 0.2 mL TritonX-100, and heating until no precipitates. The mixture solution was re-dispersed in 1.6 mL GBS and stored at 4 °C for future use.

2.2 Apparatus

All electrochemical measurements were performed on a CHI660D electrochemical workstation (Shanghai Chenhua Instrument Corporation, Shanghai, China) at room temperature (RT). A conventional screen-printed electrode system (SPE, Nanjing Yunyou Biotech Co., Ltd, China) was used for all electrochemical measurements: one carbon paste electrode as the working electrode, another carbon paste electrode as the auxiliary electrode and Ag/AgCl electrode as the pseudoreference electrode. Cyclic voltammetry (CV) was performed in phosphate buffer saline (PBS, pH 7.4, 0.1 mol/L Na_2HPO_4/KH_2PO_4 and 0.1 mol/L NaCl) containing 5 mmol/L $K_3Fe(CN)_6/K_4Fe(CN)_6$ and 0.1 mol/L KCl between -0.3 and 0.6 V with a scanning rate of 100 mV/s. Linear sweep voltammetry (LSV) was carried out in 0.1 mol/L HNO_3 solution containing 0.6 mol/L KNO_3 and 0.1 mol/L KCl from -0.1 V to 0.6 V with a scanning rate of 100 mV/s according to the previous report (Chu, et al. 2005).

The morphologies and surface structures of the prepared cholesterol biosensor were characterized with scanning electron microscope (SEM), X-ray photoelectron spectroscopy (XPS) and Raman spectra. SEM images were obtained from a Quanta 200 field environmental scanning electron microscope (FEI COMPANY, USA). XPS was performed using an ESCALAB 250Xi

spectrometer (Thermo-Fisher, USA). During the analysis process, the Mg cathode radiation source of 1253.6 eV was used at the conditions of 10 mA and 15 keV with a pass energy of 40 eV and the residual pressure in the chamber was 10^{-7} Pa. Raman spectra were measured on a DXR Raman microscope (Thermo-Fisher Scientific, USA)

2.3 Preparation of GO&CHER&CHOD mixture enzyme solution

GO (3.0 mg) was added into 3.0 mL ultrapure water and ultrasonic dispersed uniformity for 2 h to obtain 1.0 mg/mL of GO suspension. Then, 4.0 mL of 10.0 mmol/L EDC solution and 1.0 mL of 10.0 mmol/L NHS solution were added into the 3.0 mL GO suspension and incubated for 1 h at RT. Then, 100 μL CHER solution (1.0 mg/mL) and 100 μL CHOD solution (1.0 mg/mL) were added into 200 μL of the above GO suspension solution. Finally, the GO&CHER&CHOD mixture enzyme solution was incubated at 4 °C for 3 h and stored at -20 °C for future use.

2.4 Preparation of cholesterol biosensor

The bare SPE was treated in 0.5 mol/L H_2SO_4 by CV for 10 cycles between -0.2 and 1.0 V with a scanning rate of 100 mV/s. Then, Au NPs was deposited onto the activated SPE through the constant potential deposition in 5.0 mL of 0.01% $HAuCl_4$ solution at RT under a constant potential of -0.5 V for 120 s while the magnetic stirring. After the electrode was cleaned with water and dried at RT, 2.0 μL of the GO&CHER&CHOD mixture enzyme solution was dropped onto the surface of Au NPs/SPE and incubated for 1 h at 4 °C in a moisture environment. After that, the electrode was rinsed with GBS to remove the unbound GO&CHER&CHOD. Thus, the cholesterol biosensor (GO&CHER&CHOD/Au NPs/SPE) was came into being and stored at 4 °C for further use.

2.5 Electrochemical detection of cholesterol

Different concentration of cholesterol solution (2.0 μL) and 1.5 μL of $AgNO_3$ solution (90 mmol/L) were added to the surface of the cholesterol biosensor. After incubated for 1 h in the dark at

37 °C, the electrode was washed twice with GBS at RT. Then, LSV was performed to record the anodic stripping peak current of Ag in 0.1 mol/L HNO_3 solution containing 0.6 mol/L KNO_3 and 0.1 mol/L KCl between -0.1 and 0.6 V with a scanning rate of 100 mV/s.

3. Results and discussion

3.1 Analytical principle of the electrochemical biosensor for cholesterol detection

Scheme 1 described the working principle of the electrochemical cholesterol biosensor based on GO and Au NPs co-mediated enzymatic Ag deposition. Firstly, The CHOD and CHER were conjugated to GO via the formation of amide using EDC/NHS as crosslinking agent (Scheme 1A). Then, Au NPs was deposited on the surface of the SPE by potentiostatic electro-deposition. After that, GO&CHER&CHOD mixture enzyme was immobilized on the surface of Au NPs-modified SPE by electrostatic adsorption. In the presence of cholesterol, the CHER&CHOD immobilized on sensor electrode catalyzed the oxidization of cholesterol to generate cholest-4-en-3-one and H_2O_2. Subsequently, the Ag ion in the solution was reduced to metallic Ag which deposited on the surface of Au NPs modified SPE by H_2O_2 in the presence of GO and Au NPs. The deposited Ag produced a detectable anodic stripping signal, which could be determined by LSV. The LSV current is directly proportional to the concentration of H_2O_2, which is derived from cholesterol. Therefore, by measuring LSV current, cholesterol can be detected with high sensitivity (Scheme 1B).

(Here Scheme 1)

3.2 Amplification performance of the electrochemical cholesterol biosensor

In order to verify the amplification performance of the electrochemical cholesterol biosensor, LSV response with and without the addition of cholesterol were recorded and the results were shown

in Fig. 1A. There was a remarkable current response (496.7 μA) at 200 mV on the GO&CHER&CHOD/Au NPs/SPE in the presence of cholesterol (Fig. 1A, curve a). Compared with curve a, a mild current response (260.7 μA) appeared at 185 mV on the CHER&CHOD/Au NPs/SPE with the presence of cholesterol (Fig. 1A, curve b). This could be reasoned that GO and Au NPs could co-mediate enzymatic Ag deposition which would produce an amplified signal. As a control, there was a current response (145.9 μA) at 159 mV on the GO&CHER&CHOD/Au NPs/SPE with the presence of BSA (Fig. 1A, curve c), indicating that the prepared cholesterol sensor has a good specificity. Without the presence of cholesterol, the GO&CHER&CHOD/Au NPs/SPE could not produce H_2O_2 and the reduce reaction could not be implemented, and there was a nunconspicuous current peak of 109.8 μA at 152 mV (Fig. 1A, curve d). Due to the phenomenon of the underpotential deposition (Langille et al. 2012), there was a weak current response (72.9 μA) at 144 mV on the Au NPs/SPE with the presence of cholesterol (Fig. 1A, curve e). Hence, the biosensor showed a good sensitivity and specificity, so it can be used to detect cholesterol effectively.

3.3 Electrochemical characterization of cholesterol biosensor

CV was used to observe the changes of electrochemical behavior at different stages of cholesterol biosensor. The CV behavior of the various modification stages of the SPE were shown in Fig. 1B. A reversible redox peak appeared with bare SPE and an oxidation peak current with 46.23 μA was observed, which due to the equivalent amount of $Fe(CN)_6^{4-}$ and $Fe(CN)_6^{3-}$ ions in the reaction medium (Fig. 1B, curve a). After deposition of Au NPs on the surface of SPE, the redox peak increased obviously, and the magnitude of the oxidation peak current increased to 92.55 μA (Fig. 1B, curve b). This was due to the good conductivity of Au NPs on the surface of the electrode, which is favorable for the electron transfer. However, the CV of GO&CHER&CHOD/Au NPs/SPE

showed an oxidation peak current of 57.53 μA (Fig. 1B, curve c), less than the Au NPs/SPE current (92.55 μA), which may be attributed to the insulating nature of the covalently attached CHER&CHOD molecules. This was because the enzyme belongs to the class of protein and the conductivity of the enzyme is weak. Compared with the curve c, the redox peak of the Ag/GO&CHER&CHOD/Au NPs/SPE (Fig. 1B, curve d) increased obviously. The higher value of the oxidation peak current (78.42 μA) obtained for Ag/GO&CHER&CHOD/Au NPs/SPE was due to the conductivity of metallic Ag. The cholesterol was decomposed and produced the H_2O_2, by which the Ag ions were reduced to metallic Ag that deposited on the surface of Au NPs/SPE. Due to the conductivity of Ag, the redox peak of curve d was larger than that of curve c.

The average value of the electroactive surface area could be calculated according to the Randles-Sevcik equation from references (Bai et al. 2016; Tig et al. 2016).

$$Ip=2.69\times10^{5}AD^{1/2}\,n^{3/2}\,\gamma^{1/2}C \qquad (1)$$

The Ip indicates the current peak value, A represents the effective area of the electrode surface (cm^2), D on behalf of the diffusion coefficient of the $[Fe(CN)_6]^{3-/4-}$molecule ($D=6.70 \pm 0.02\times10^{-6}$ cm^2/s), n represents the number of electrons participating in the redox reaction (for $[Fe(CN)_6]^{3-/4-}$, n=1), γ represents the scan rate of the potential perturbation ($V\cdot s^{-1}$), and C is the bulk concentration of the redox probe ($mol\cdot cm^{-3}$). And n indicates the number of electrons involved in redox reactions (n=1), γ is the change rate of voltage (0.1 $V\cdot s^{-1}$).

By calculation, the effective surface area of the screen printed working electrode was bare SPE (0.1342 cm^2) < GO&CHER&CHOD/Au NPs/SPE (0.1646 cm^2) < Ag/GO&CHER&CHOD/Au NPs/SPE (0.2258 cm^2) < Au NPs/SPE (0.2584 cm^2). These results showed that the eletro-deposition of Au NPs was beneficial to increase the surface area of the working electrode.

(Here Fig. 1)

3.4 SEM characterization of cholesterol biosensor

Fig. S1 (Supporting Information) showed the SEM characterization of the stepwise modification process of cholesterol biosensor. Fig. S1A was the SEM image of the bare SPE, the surface of the electrode was more evenly distributed and there was no obvious particle distribution. After depositing Au NPs by constant potential, the SEM image was shown in Fig. S1B. It can be seen that a layer of particles evenly distributed in the electrode surface, which showed the surface of the electrode has been successfully deposited Au NPs. Fig. S1C was the SEM image of GO&CHER&CHOD mixture enzyme solution immobilized on the surface of Au NPs/SPE. It can be seen that there was a black layer between the particles. Compared to Fig. S1B and Fig. S1C, the SEM image of Ag/GO&CHER&CHOD/Au NPs/SPE (Fig. S1D) had smaller particles and the layered objects were also decreased, indicating that Ag ions in $AgNO_3$ solution had been reduced to metallic Ag and deposited on the electrode surface.

3.5 Raman characterization of cholesterol biosensor

Raman spectroscopy is a ubiquitously practiced technique for distinguishing between sp^2 and sp^3 hybridization in carbonaceous materials. Fig. S1E showed the Raman spectroscopy for different stages of SPE modification. Seen from Fig. S1E, two main characteristic Raman bands can be seen obviously at 1352 cm^{-1} (D-band) and 1591 cm^{-1} (G-band).The intensity of D-band and G-band of GO&CHER&CHOD/AuNPs/SPE (curve c) was higher than that of SPE (curve a), AuNPs/SPE (curve b) or Ag/GO&CHER&CHOD/AuNPs/SPE (curve d). Since the electric signal of the SPE immobilized enzymes and GO was significantly larger than that of the other three electrodes, this can be explained that GO has been successfully immobilized on the electrode surface.

3.6 XPS characterization of cholesterol biosensor

XPS was further used to estimate effective information on the chemical composition for different stages of SPE modification. Five main features including C1s, N1s, O1s, Au4f and Ag3d peaks of the XPS spectrum were inspected. Fig. S2A was the full XPS spectrum of all elements in different stages of SPE modification. It can be seen from Fig. S2A that a higher intensity C1s (284 eV), O1s (531 eV) associated with lower intensity peak series of N1s (399 eV), Au4f (83 eV). Moreover, the presence of Ag3d (367 eV) was related to lower intensity peak series of N1s (399 eV) and Au4f (83 eV).

Fig. S2B showed the XPS characterization of different elements (C1s，N1s，O1s，Au4f) at different stages of electrode modification process. Compared to the curve a in Fig. S2B, the signals of C1s (284 eV), N1s (399 eV) and O1s (531 eV) decreased as the Au4f (83 eV) signal appeared (Fig. S2B, curve b). This was due to the deposition of Au NPs on the surface of SPE. Moreover, the signal intensity of C1s (284 eV), O1s (531 eV) and N1s (399 eV) in curve c in Fig. S2B increased obviously, while the signal intensity of Au4f (83 eV) was significantly weaken. This is because CHER, CHOD and GO were immobilized on the surface of Au NPs/SPE. Subsequently, the signal intensity of C1s (284 eV), N1s (399 eV) and Au4f (83 eV) decreased significantly with the presence of Ag3d (367 eV) signal (Fig. S2B, curve d), due to the deposition of metallic Ag onto the surface of Au NPs/SPE.

A further insight on the reaction process can be obtained from the inspection of Table inset Fig. S2A, where the relative abundance (% of atoms) of the various elements (C, O, N, Au, Ag) for reaction processes are summarized. The immobilized GO&CHER&CHOD conjugates caused a strong increase in the proportion of C which is above 66% and mild increase in the proportion of O from 14.94% to 25.47%.After the deposition of metallic Ag onto the surface of Au NPs/SPE, the

proportion of Ag was 1.88%, while the proportion of Au decreased strongly from 83.84% to 1.43%.

3.7 Optimization of experimental conditions for detection cholesterol

It is important to optimize experimental conditions for the excellent performance of the cholesterol biosensor. In this paper, we optimized several key parameters such as the incubation temperature, the immobilization time of the enzyme, the concentration of GO, the concentration of Ag^+ and pH of the detection solution by single-factor experiment and the results were shown in Fig. 2.

In Fig. 2A, the current response increased with the increase of incubation temperature of enzyme and cholesterol from 4 ºC to 37 ºC and reached the peak at 37 ºC. Then, the sensor response began to decrease as the temperature continued to rise above 37 ºC. It is known that the catalytic activity of enzyme changes with temperature, when the temperature is too low, the catalytic activity of enzyme decreased and the reaction rate is low. But when the temperature is too high, enzyme will inactivate and loss of its catalytic activity. Therefore, the optimal incubation temperature of enzyme and cholesterol at 37 °C was selected for following experiments.

Immobilization time is another important parameter because it determines the amount capacity of enzymes loading on the surface of electrode. The effect of the immobilization time of the GO&CHER&CHOD mixture enzyme and cholesterol on the current response was studied by varying the immobilization time in the range from 0.5 h to 9 h at 37 °C and the results were shown in Fig. 2B. Seen from Fig. 2B, the current response of the sensor was the strongest when the immobilization time was 1 h. This was because when the time was less than 1 h, the GO&CHER&CHOD conjugates on the surface of the electrode were not completely adsorbed to the electrode surface, resulting smaller current response of the sensor. When the time was greater than 1 h, the activity of CHER and

CHOD would be decreased with the increase of the immobilization time. Therefore, 1 h was selected for the immobilization time of the GO&CHER&CHOD mixture enzyme solution in the whole experiments.

The concentration of GO in the enzyme solution is also an important parameter which affecting the current response of the sensor. The effect of GO concentration (125 - 470 μg/mL) in enzyme solutions on the current response was investigated and the results were shown in Fig. 2C. The current response of the sensor was the strongest when the concentration of GO was 200 μg/mL, and the response signal began to decrease when the concentration of GO was more than 200 μg/mL. This was because the concentration of the GO increased while the concentration of the CHER&CHOD decreased, so that the current response of the sensor decreased. Thus, the concentration of GO in the enzyme solution was chosen as 200 μg/mL in the further experiment.

Fig. 2D showed the effect of Ag^+ concentration on the current response of electrochemical cholesterol biosensor. As shown in Fig. 2D, the current response of the sensor increased with the increase of Ag^+ concentration in the range from 10 mmol/L to 90 mmol/L. The current response began to decrease with higher Ag^+ concentration, which might be attributed to the inhibition of emzyme activity by Ag^+ at high concentration. Therefore, the concentration of Ag^+ of 90 mmol/L was selected in subsequent experiments.

The pH of the reaction system is another important factor for the enzyme-catalyzed silver deposition sensor, so the suitable pH was investigated. Fig. 2E showed the changes of the current response at different pH (3.6-10.6). Seen from Fig. 2E, the current response increased with increasing pH and the strongest current response was obtained at pH 8.6, indicating that the biosensor was more active at this pH and the immobilized CHER&CHOD kept its natural structure

and did not denature. Thus, pH 8.6 was selected through the whole experiment.

(Here Fig. 2)

3.8 Analytical performance of the cholesterol biosensor

Under the optimum experimental conditions, the developed cholesterol biosensor was used to measure different concentration of cholesterol, and the current response was recorded with a linear sweep voltammetry curve (Fig. 3A). A negligible signal was observed without the addition of cholesterol, while noticeable LSV signal appeared with the addition of cholesterol. The current response increased with the increase of cholesterol concentration. Fig. 3B was the linear calibration curve of the sensor. With the concentration of cholesterol ranging from 0.01 μg/mL to 5000 μg/mL, good linearity between the LSV current and the cholesterol concentration was achieved. The linear regression equation was fitted as Y = 478.7030 + 0.0840X with the correlation coefficient of 0.9991, where Y denoted the LSV current value (μA), X was the cholesterol concentration (μg/mL). The sensitivity, expressed as the slope of the calibration straight-line section, was calculated from the plot of Fig. 3B by means of linear regression. With the help of the linear regression, the sensitivity was calculated to be 0.084 $\mu A/cm^{-2}\cdot\mu g/mL$. In addition, the limit of detection (LOD) was 0.001 μg/mL with a signal/noise (S/N) ratio of 3.

The low LOD could be attributed to the following factors. First, GO possessed high electron-transfer capability and large specific surface area to capture and immobilize more CHER&CHOD enzyme. Second, GO contributed to catalyze silver deposition reaction to improve greatly the response signal. Third was the excellent electrical conductivity of Au NPs, which may enhance the ability of electron transfer on the electrode surface.

Furthermore, the analytical performances of the proposed biosensor were compared with those cholesterol sensors, as summarized in Table 1. It could be found that the proposed biosensor exhibited good sensitivity, satisfactory detection limit and linear range.

(Here Fig. 3)

(Here Table 1)

3.9 Specificity, reproducibility and stability of the cholesterol biosensor

Specificity was investigated by the Ag/GO&CHER&CHOD/Au NPs/SPE under the same conditions, and different common interfering substances were used, e.g. glucose, DL-cysteine, ascorbic acid, BSA and uric acid. As can be seen from Fig. 3C, current response of the prepared cholesterol sensor with cholesterol, glucose, DL-cysteine, ascorbic acid, BSA and uric acid were 900.55 μA, 62.32 μA, 92.51 μA, 123.20 μA, 126.00 μA and 191.00 μA, respectively. These current responses were account for 6.92%, 10.27%, 13.68%, 13.99%, 21.21% of the corresponding signal of cholesterol. The results showed that these compounds produced little interference when the distractors were used to replace cholesterol. Hence, the biosensor had a high specific affinity for cholesterol detection.

The reproducibility of the electrochemical biosensor was investigated by detecting the same concentration of cholesterol (250 μg/mL) with intra-assay imprecision of six different sensors under the same condition and inter-assay imprecision at six different assays. The LSV responses were evaluated. The mean of the current response value was 480.52 μA. The relative standard deviation (RSD) of the intra-assay and inter-assay precisions of the cholesterol biosensor were 3.86% and 4.95%, respectively, which implied the acceptable reproducibility of the proposed cholesterol biosensor for potential practical applications.

To check the operational stability of this biosensor, the electrochemical performance of Ag/GO&CHER&CHOD/Au NPs/SPE was tested against the storage time. The present cholesterol biosensor was stored in a humid environment at 4 °C when the sensors were out of use. LSV measurements were performed in the presence of cholesterol (250 μg/mL). The current response of Ag/GO&CHER&CHOD/Au NPs/SPE was almost stable in first 3 days (505.34 ± 8.15 μA, n=6), after that it began to decrease slowly. A 3.15% decrease in the current response was observed after 3

days and a 8.85% decrease after 7 days. Eventually the current response (437.52 ± 6.32 μA, n=6) retained 86.58% of the original value after 15 days. The results suggested that the constructed LSV detection method exhibited good stability for the cholesterol determination.

3.10 Recovery of the cholesterol biosensor

In order to test the recovery rate of the sensor, we detected the sensor response towards different concentration of the cholesterol (4000 μg/mL, 2000 μg/mL, 800 μg/mL, 200 μg/mL, 80 μg/mL), and the results were shown in Table 2. As can be seen from Table 2, the recovery rate was from 97.0% to 106.79%. The satisfying results demonstrated that the biosensor had a great potential for practical application.

(Here Table 2)

4. Conclusions

In summary, a new electrochemical biosensor with high sensitivity for cholesterol monitoring based on GO and Au NPs co-mediated enzyme catalyzed Ag deposition was designed by immobilizing GO&CHER&CHOD conjugates onto the surface of Au NPs modified SPE. The synergistic effect of CHER&CHOD, GO and Au NPs provided excellent catalytic ability for cholesterol hydrolyzing to generate H_2O_2, which can reduce the Ag ions in the solution to metallic Ag and deposited on the surface of Au NPs modified SPE, and thus efficiently amplifying the LSV current signal for cholesterol detection. Experimental results showed that the developed electrochemical cholesterol biosensor was of excellent performances, such as wide liner range, low LOD, good recovery, high specificity, acceptable reproducibility and stability. This new cholesterol biosensor might offer great potential in assaying cholesterol in clinical samples in the future.

Acknowledgments

This work was supported by the National Nature Science Foundation of China (Nos. 81430055, 81372362 and 81460451), Program for Changjiang Scholars and Innovative Research Team in University of Ministry of Education of China (No. IRT_15R13), the Innovation Project of Graduate Education (2017YJCX95, YCSW2017146), the Post doctoral Research Fund of China (Nos. 2013T60830 and 2013M531916) and the National Science Foundation of Guangxi province of China (Nos. 2015GXNSFDA139025, 2016GXNSFAA380011 and 2016GXNSFAA380080).

References

Abraham, S., Srivastava, S., Kumar, V., Pandey, S., Rastogi, P.K., Nirala, N.R., Kashyap, S., Srivastava, S.K., Singh, V.N., Ganesan, V., Saxena, P.S., Srivastava, A., 2015. J. Electroanal. Chem. 757, 65-72.

Alexander, S., Barapeedharan, P., Balasubrahmanyan, S., Ramaprabhu, S., 2017. Eur. Polym. J. 86, 106-116.

Bai, Z.H., Li, G.Y., Liang, J.T., Su, J., Zhang, Y., Chen, H.Z., Huang, Y., Sui, W.G., Zhao, Y.X., 2016. Biosens. Bioelectron. 82, 185-194.

Batra, N., Tomar, M., Gupta, V., 2015. Biosens. Bioelectron. 67, 263-271.

Bo, X.J., Zhou, M., Guo, L.P., 2017. Biosens. Bioelectron. 89, 167-186.

Bui, T.T., Park, S.Y., 2016. Green Chem. 18(15), 4245-4253.

Cao, S.R., Zhang, L., Chai, Y.Q., Yuan, R., 2013. Biosens. Bioelectron. 42, 532-538.

Chen, J., Jackson, A.A., Rotello, V.M., Nugen, S.R., 2016. Small 12(18), 2469-2475.

Chu X., Fu X., Chen K., Shen G. L., Yu R. Q., 2005. Biosens. Bioelectron. 20, 1805-1812.

Conzuelo, F., Grutzke, S., Stratmann, L., Pingarron, J.M., Schuhmann, W., 2016. Microchim. Acta 183(1), 281-287.

Gao, N.N., Gao, F., He, S.Y., Zhu, Q.H., Huang, J.F., Tanaka, H., Wang, Q.X., 2017. Anal. Chim. Acta. 951, 58-67.

Halder, A., Zhang, M., Chi, Q., 2017. Biosens. Bioelectron. 87, 764-771.

Huang, Y., Cui, L.J, Xue, Y.W, Zhang, S.B., Zhu, N.X., Liang, J.T., Li, G.Y., 2017. Mater. Sci. Eng. C 77, 1-8.

Jiaul Haque, A.M., Kim, J., Dutta, G., Kim, S., Yang, H., 2015. Chem. Commun. 51(77),

14493-14496.

Khatun, R., Hunter, H., Magcalas, W., Sheng, Y., Carpick, B., Kirkitadze, M., 2017. Comput. Struct. Biotechnol. J. 15, 14-20.

Komathi, S., Muthuchamy, N., Lee, K.P., Gopalan, A.I., 2016. Biosens. Bioelectron. 84, 64-71.

Langille, M. R., Personick, M. L., Zhang, J., Mirkin, C. A., 2012. J. Am. Chem. Soc. 134, 14542−14554

Lee, K., Ahmed, M.S., Jeon, S., 2015. J. Power Sources 288, 261-269.

Li, R.M., Xiong, C., Xiao, Z.Y., Ling, L.S., 2012. Anal. Chim. Acta 724, 80-85.

Lin, T.R., Zhong, L.S., Chen, H., Li, Z.H., Song, Z.P., Guo, L.Q., Fu, F.F., 2017. Microchim. Acta 184(4), 1233-1237.

Lin, X.Y., Ni, Y.N., Kokot, S., 2016. Sens. Actuators B-Chem. 233, 100-106.

Nandini, S., Nalini, S., Reddy, M.B., Suresh, G.S., Melo, J.S., Niranjana, P., Sanetuntikul, J., Shanmugam, S., 2016. Bioelectrochemistry 110, 79-90.

Sharma, S., Prakash, V., Mehta, S.K., 2017. TrAC-Trends Anal. Chem. 86, 155-171.

Sharma, V., Mobin, S.M., 2017. Sens. Actuators B 240, 338-348.

Tig, G.A., Zeybek, D.K., Pekyardimci, S., 2016. Chem. Pap. 70(6), 695-705.

V, C.S., Berchmans, S., 2016. Mater. Sci. Eng. C. 64, 183-189.

Wan, Y., Wang, Y., Wu, J.J., Zhang, D., 2011. Anal. Chem. 83(3), 648-653.

Yang, L., Zhao, H., Li, Y.C., Ran, X., Deng, G.G., Zhang, Y.Q., Ye, H.Z., Zhao, G.F., Li, C.P., 2016. Analyst 141(1), 270-278.

Yang, X., Gao, Z., 2015. Chem. Commun. 51(32), 6928-6931.

Yee, M.S., Khiew, P.S., Chiu, W.S., Tan, Y.F., Kok, Y.Y., Leong, C.O., 2016. Colloid. surface. B

148, 392-401.

Zheng, Y.H, Wang, A.W., Cai, W., Wang, Z., Peng, F., Liu, Z., Fu, L., 2016. Enzyme. Microb. Tech. 95, 112-117.

Figure Captions

Scheme1Principle of the electrochemical detection of cholesterol based on GO and Au NPs co-media ted enzymatic Ag deposition.

Fig. 1 (A) LSV curves of (a) the GO&CHER&CHOD/Au NPs/SPE in the presence of cholesterol, (b) the CHER&CHOD/Au NPs/SPE in the presence of cholesterol, (c) the GO&CHER&CHOD/Au NPs/SPE in the presence of BSA, (d) the GO&CHER&CHOD/Au NPs/SPE without the presence of cholesterol, (e) the Au NPs/SPE in the presence of cholesterol. The concentration of cholesterol was 2.0 mg/mL and the current signal was obtained by the LSV. (B) CV curves of (a) bare SPE, (b) Au NPs/SPE, (c) GO&CHER&CHOD/Au NPs/SPE, and (d) Ag/GO&CHER& CHOD/Au NPs/SPE.

Fig. 2 (A) Effect of incubation temperature on the current response. (B) Effect of immobilization time of enzyme on the current response. (C) Effect of concentration of GO on the current response. (D) Effect of concentration of Ag^{+} on the current response. (E) Effect of pH on the current response. The concentration of cholesterol in this experiment is 1.5 mg/mL and the current response was obtained by the LSV. The error bars represent the relative standard deviation (n = 3 electrodes).

Fig.3 (A) LSV curve of different level cholesterol including 5000 μg/mL, 3000 μg/mL, 1000 μg/mL, 500 μg/mL, 50 μg/mL, 0.01 μg/mL, 0 μg/mL. (B) Working curve of the cholesterol biosensor. (C) Specificity of the proposed biosensor with glucose, DL-cysteine, ascorbic acid, BSA, uric acid instead of cholesterol. The error bars represent the relative standard deviation (n = 3 electrodes).

Table 1 Comparison of analytical performance with some other biosensors for detection of cholesterol

Electrode or matrix	Method	Liner range	sensitivity	LOD	Reference
(ChEt-ChOx)/(ZnO-CuO)/ITO/glass bioelectrode	CV	0.5 - 12 mM	760 mA/cm^2·mM		(Batra et al. 2015)
Nafion/SnO_2NPs-ChOx/CPE	Amperometry	0.20 - 4.95 μM		0.04 μM	(Tig et al. 2016)
ChOx/Nafion/Bi-Pt	Amperometry	0.05 - 22 mM	3.41 μA/cm^2·mM	50 μM	(V and Berchmans 2016)
[a]G/Ti(G) 3DNS/CS/ ChOxbioelectrode	Amperometry	0.05 - 8.0 mM	3.82 μA/cm^2·mM	6 μM	(Komathi et al. 2016)
Nafion/Chox/MoS_2-AuNPs/ GCE	Amperometry	0.5 - 48 μM	4460 μA/cm^2·mM	0.26 μM	(Lin et al. 2016)
[b]ChOx /AuNs/GO-SH/Gr	Amperometry	0.05 - 11.45 mM	273 mA/cm^2·mM	0.2 nM	(Nandini et al. 2016)
[c]ChOx/AuNPs/TGHs/TGPHs /GCE	Amperometry	0.05-590 μM		0.017 mM	(Cao et al. 2013a)
[d] MB-bound CX6–Gra/GCE	DPV	0.50 - 50.00 μM	0.099 μA/μM	0.20 μM	(Yang et al. 2016)
Ag/GO&CHER&CHOD/Au NPs/SPE	LSV	0.01 - 5000 μg/mL	0.084 μA/cm^{-2}·μg/mL	0.001 μg/mL	This work

[a]Graphene (G) sheets interconnected-graphene embedded titanium nanowires (TiO_2(G)-NWs) 3D nanostacks (G/Ti(G)3DNS); chitosan (CS)

[b] Gr: Graphite; GO-SH: thiol-functionalized graphene oxide; AuNs: gold nanostructure

[c] TiO_2-graphene-Pt-Pd hybrid materials (TGPHs); TiO_2-graphene hybridmaterials (TGHs)

[d] 4-sulfocalix[6]arene hydrate (CX6); calix[6]arene functionalized graphene (CX6–Gra); methylene blue (MB)

Table 2 Determination of cholesterol by the proposed electrochemical biosensor

Concentration Added (μg/mL)	Measured Current (μA)	Concentration Found (μg/mL)	Recovery (%)
4000	801.04 ± 14.03	3842.02 ± 167.07	102.00%
2000	641.27 ± 4.01	1940.00 ± 47.74	97.00%
800	543.80 ± 9.62	779.72 ± 71.45	97.46%
200	494.78 ± 2.15	196.11 ± 25.58	98.05%
80	485.48 ± 6.12	85.43 ± 7.29	106.79%

Figures

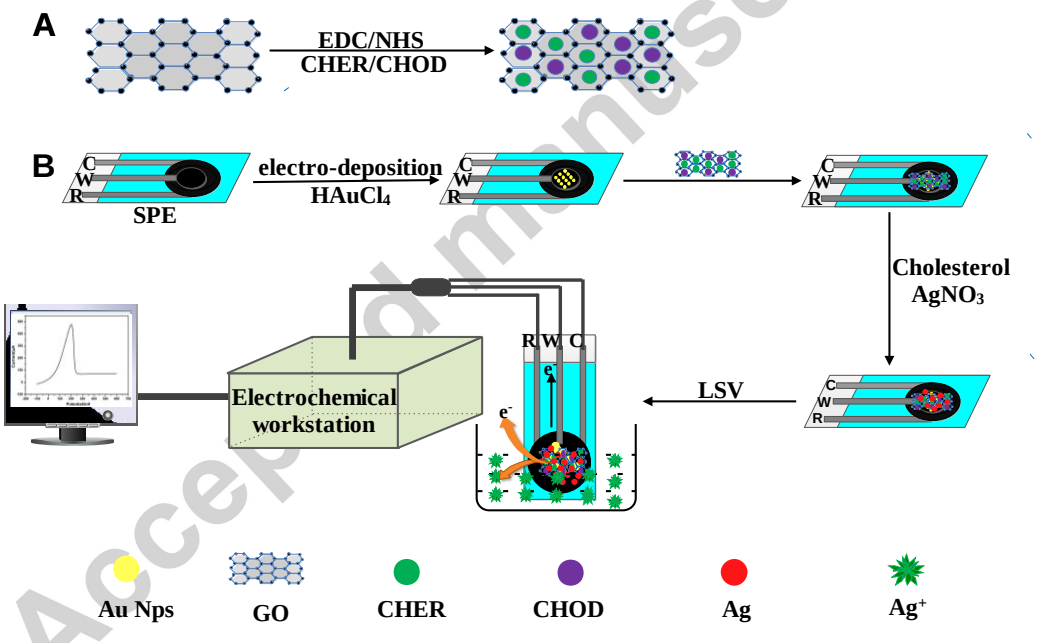

Scheme.1

Fig.1

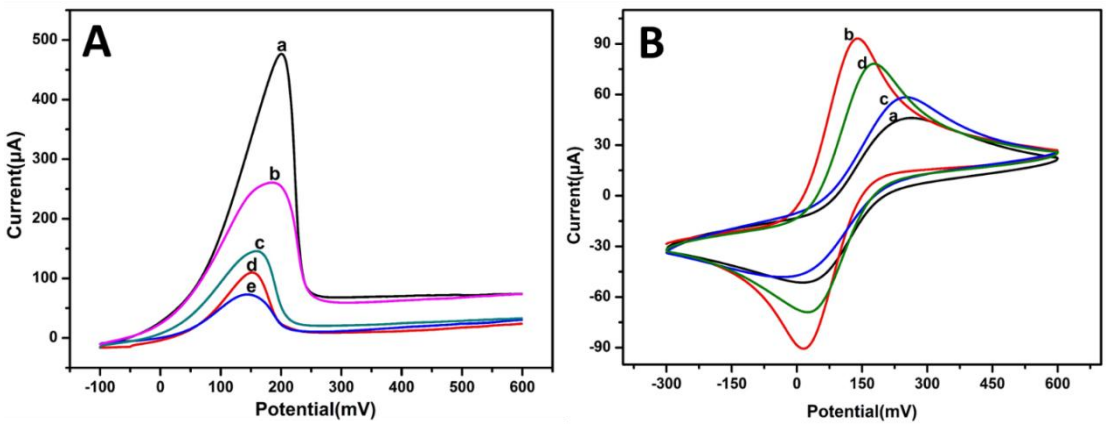

Fig .2

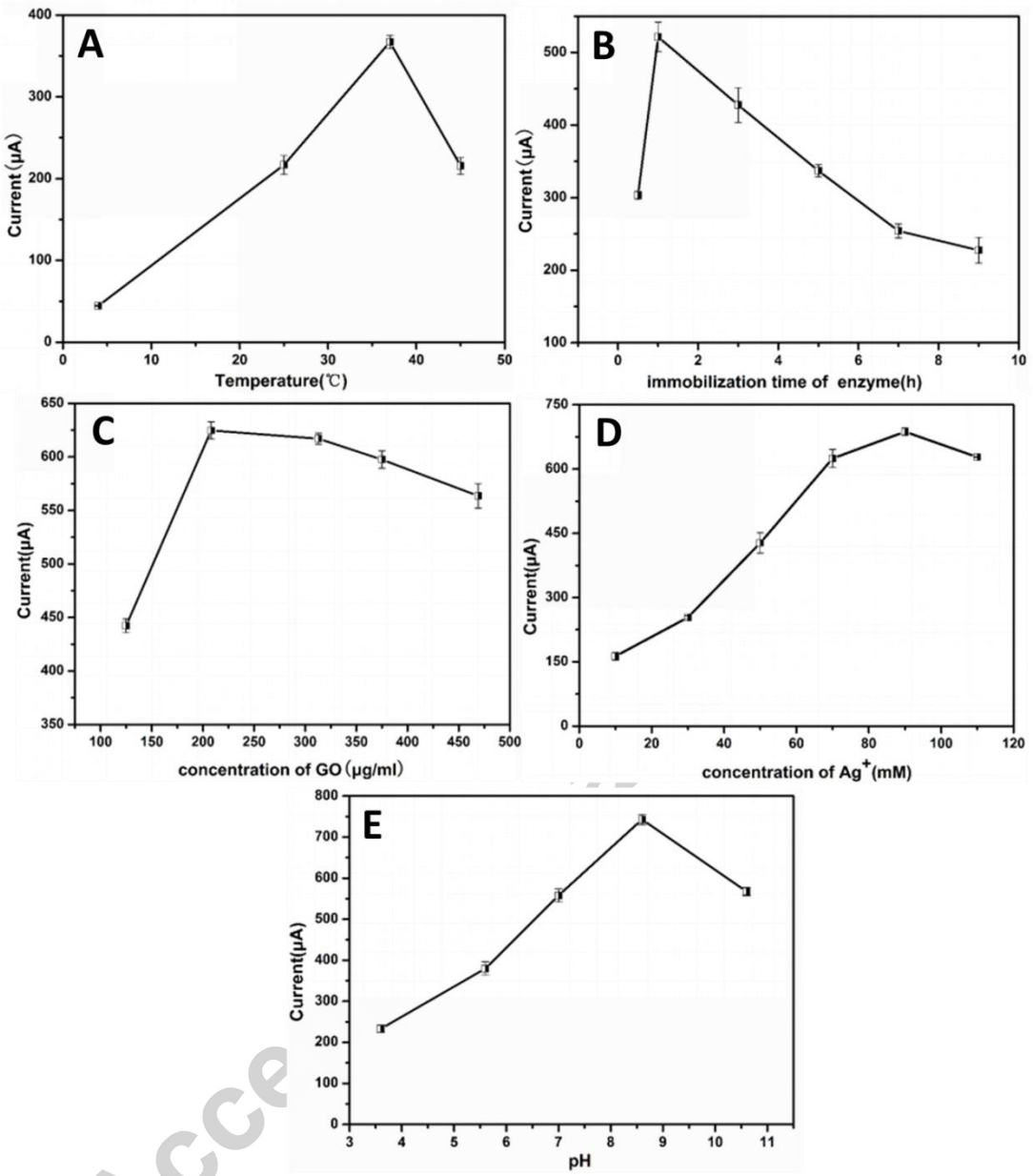
A
Current (μA)
Temperature(℃)
B
Current (μA)
immobilization time of enzyme(h)
C
Current(μA)
concentration of GO (μg/ml)
D
Current(μA)
concentration of Ag+(mM)
E
Current(μA)
pH

Fig .3

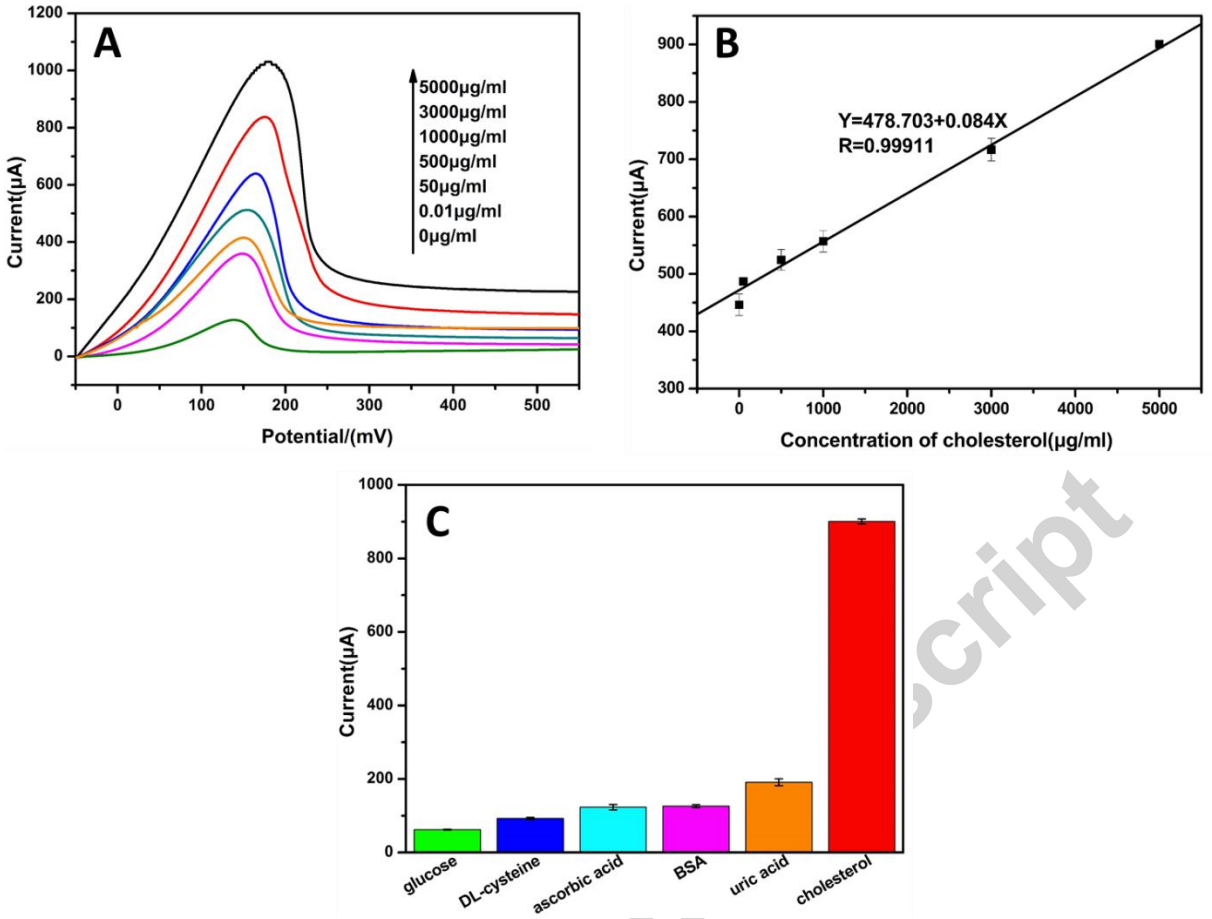

Highlights

1. A simple and ultrasensitive cholesterol biosensor based on graphene mediated enzymatic silver deposition was developed.
2. GO possessed high electrontransfer capability and large specific surface area to capture and immobilize more CHER&CHOD enzyme.
3. GO contributed to catalyze silver deposition reaction to improve greatly the response signal.
4. The low detection limit of 0.001 μg/mL (2.6 nmol/L) was obtained at the signal/noise (S/N) ratio of 3.
5. The ultrasensitive cholesterol biosensor exhibited higher specificity, acceptable reproducibility.